Journal of Medicinal Chemistry

Article

Combination of L-carnitine with lipophilic linkage-donating gemcitabine derivatives as intestinal novel organic cation transporter 2-targeting oral prodrugs

Gang Wang, Hong-xiang Chen, Dong-yang Zhao, Da-wei Ding, mengchi Sun, Long-fa Kou, Cong Luo, Dong Zhang, Xiu-lin Yi, Jinhua Dong, Jian Wang, Xiaohong Liu, Zhonggui He, and Jin Sun

J. Med. Chem., **Just Accepted Manuscript** • DOI: 10.1021/acs.jmedchem.7b00049 • Publication Date (Web): 24 Feb 2017

ACS Publications

Journal of Medicinal Chemistry is published by the American Chemical Society. 1155 Sixteenth Street N.W., Washington, DC 20036

Combination of L-carnitine with lipophilic linkage-donating gemcitabine derivatives as intestinal novel organic cation transporter 2-targeting oral prodrugs

Gang Wang[a], Hongxiang Chen[a], Dongyang Zhao[a], Dawei Ding[a], Mengchi Sun[a], Longfa Kou[a], Cong Luo[a], Dong Zhang[a], Xiulin Yi[c], Jinhua Dong[a], Jian Wang[d], Xiaohong Liu[a], Zhonggui He[a] and Jin Sun[a,b]*

[a] School of Pharmacy, Shenyang Pharmaceutical University, Wenhua Road, Shenyang 110016, China

[b] Municipal Key Laboratory of Biopharmaceutics, School of Pharmacy, Shenyang Pharmaceutical University, China

c State Key Laboratory of Drug Delivery Technology and Pharmacokinetics, Tianjin Institute of Pharmaceutical Research, Tianjin, China

d Key Laboratory of Structure-Based Drug Design and Discovery, Shenyang Pharmaceutical University, Ministry of Education, China

KEYWORDS: gemcitabine; new organic cation transporter 2 (OCTN2); prodrug; bioavailability.

ABSTRACT

The novel organic cation transporter 2 (OCTN2, *SLC22A5*) is responsible for the uptake of carnitine through the intestine and, therefore, it may be a promising molecular target for designing oral prodrugs. Poor permeability and rapid metabolism have greatly restricted the oral absorption of gemcitabine. We here describe the design of intestinal OCTN2-targeting prodrugs of gemcitabine by covalent coupling of L-carnitine to its N4-amino group via different lipophilic linkages. Due to high OCTN2 affinity, the hexane diacid-linked prodrug demonstrated significantly improved stability (3-fold), cellular permeability (15-fold), and then increased oral bioavailability (5-fold), while causing no toxicity as compared to gemcitabine. In addition, OCTN2-targeting prodrugs can simultaneously improve the permeability, solubility and metabolic stability of gemcitabine. In summary, we present the first evidence that OCTN2 can act as a new molecular target for oral prodrug delivery and, importantly the linkage carbon chain length is a key factor in modifying the substrate affinity toward OCTN2.

INTRODUCTION

Gemcitabine is a nucleoside analog that has been used as the first-line chemotherapy for pancreatic and non-small-cell lung cancers[1]. Recently, a number of gemcitabine-based therapies in combination with cytotoxins or molecularly targeted agents began to be evaluated in clinical trials for the treatment of many cancers[2]. The antitumor activity of gemcitabine is elicited by inhibition of ribonucleotide reductase and DNA synthesis[3]. Despite therapeutic effectiveness, the administration of modality gemcitabine is currently limited to the intravenous route, which leads to poor compliance and a number of safety issues[4]. In addition, rapid kidney excretion and extensive deamination by cytidine deaminase (CD) in blood and liver result in its short half-live and need for frequent administration. Consequently, there is an urgent need to develop high-efficacy, low-toxicity oral gemcitabine products. However, so far, there are no oral preparations commercially available for gemcitabine, due to its poor membrane permeability and low metabolic stability.

Recently, a lipophilized prodrug strategy has been used to improve metabolic stability and membrane permeability[5]. The valproate amide prodrug of gemcitabine (Figure 1b) exhibited excellent stability in hepatic and intestinal homogenates and reduced deaminated metabolites (2', 2'-difluoro-2'deoxyuridine, dFdU) by 50 %, in comparison with gemcitabine. Moreover, the systemic exposure of gemcitabine (AUC) increased 1.4-fold after oral administration. The general advantages of this method include altered transport across cell membranes via passive diffusion, and a lower susceptibility to inactivation by CD. However, the poor aqueous solubility generally

limits its oral absorption and clinical application. Accordingly, carrier prodrug strategy is more recommended due to the good aqueous solubility and improved membrane permeability mediated by transporters. A series of amino acid ester prodrugs of gemcitabine were synthesized to target intestinal peptide transporter 1 (PepT1)[6, 7]. The L-valyl (Figure 1c) and D-phenylalanyl (Figure 1d) prodrugs exhibited increased Caco-2 cells permeability by 4.0-fold and 4.5-fold, respectively. However, no in vivo oral pharmacokinetic results for these prodrugs have been reported, probably due to the fact that the rapid hydrolysis to the parent drug in the gastrointestinal (GI) tract strongly limits in vivo efficacy. To obtain more stable PepT1-targeting prodrugs of gemcitabine, a number of aminoacyl amide derivatives of gemcitabine were synthesized and evaluated (Figure 1i)[8]. However, rapid rearrangement to the corresponding carboxamide occurred in aqueous solution at near neutral pH, resulting in the active parent drug being unable to be released from the prodrugs (Figure 1j). Hence, it is essential to simultaneously optimize membrane permeability, stability, and solubility for oral prodrugs of gemcitabine.

The novel organic cation transporter 2 (OCTN2, *SLC22A5*) is an important nutrient transporter to transport carnitine in small intestine, which serves as a shuttle for the transport of long-chain fatty acids into mitochondria. OCTN2 is an attractive target for the transport of carnitine analogues[9]. Two excellent examples of OCTN2-targeting prodrugs are prednisolone[10] and nipecotic[11]. Following conjugation to L-carnitine, these prodrugs are recognized by OCTN2 and exhibit increased delivery to human bronchial epithelial cells and brain following intra-tracheal

instillation and intra-peritoneal administration, respectively. More importantly, L-carnitine prodrugs significantly increase efficacy in the treatment of asthma and tonic convulsions. OCTN2 is highly expressed throughout small intestine segments, and thus represents a good target for the design of oral prodrugs[12]. To the best of our knowledge, no reports have been published in terms of OCTN2-targeting oral prodrug strategy, involving gemcitabine.

The present study mainly aimed to evaluate the usefulness of OCTN2-targeting oral prodrug strategy, and investigate the effect of the fatty acid linkage chain length (n=4-10) on the substrate affinity toward OCTN2. Four OCTN2-targeting oral prodrugs of gemcitabine, differing in the carbon chain length of the fatty acid linkage, and a non-targeting prodrug were designed and synthesized. L-carnitine was conjugated with the N4-amino group of gemcitabine since the amide bond is stable to chemical and enzymatic hydrolysis. Also, importantly, GI tract-stable prodrugs will maximize the utility of OCTN2 activity and reduce the cytotoxicity of gemcitabine exposure to the enterocytes. As expected, gemcitabine OCTN2-targeting prodrugs showed excellent stability in the GI tract and high permeability. Interestingly, the hexane diacid linkage prodrug showed better OCTN2 affinity and oral bioavailability than the other targeted prodrugs with different linkage.

RESULTS AND DISCUSSION

Design and Synthesis OCTN2-targeting oral prodrugs

Firstly, four OCTN2-targeting oral prodrugs, L-carnitine-succinic-gemcitabine (GSC), L-carnitine-hexylic-gemcitabine (GHC), L-carnitine-octanedioic-gemcitabine (GOC) and L-carnitine-decanedioic-gemcitabine (GDC) were prepared using the synthetic approach shown in Figure 2A. To evaluate the uptake mechanism of the targeted prodrugs, palmitoyl-L-carnitine (PC), a carnitine analogue but not substrate of OCTN2, was synthesized using the synthetic approach of the targeted prodrugs. Additionally, one non-targeting lipophilic amide prodrug, succinic-gemcitabine (GS), was synthesized as a negative control and was shown in Figure 2B. L-carnitine was attached to the N4-amino group of gemcitabine through fatty acid with different chain length. The 3'-hydroxyl group of L-carnitine was chosen as a conjugation site since it is a non-essential group for the carnitine interaction with OCTN2[13]. All the prodrugs were fully characterized by HPLC, MS and NMR. Detailed synthetic procedures, yields, and HPLC purity could be found in the Experimental section and Supporting information.

Stability Studies

To target intestinal transporter, the prodrugs should be stable in the GI tract after oral administration. The chemical stability was examined in different pH phosphate buffers and the half-lives ($t_{1/2}$) were obtained from linear regression of pseudo-first-order kinetics. As reflected in Table1, GSC, GHC and GS underwent slow hydrolysis at pH 1.2 and were more stable in pH 6.8-7.4 buffers. The enzymatic

stability was studied in tissue homogenates and plasma. The $t_{1/2}$ values of those prodrugs in intestinal homogenate were large, indicating that the prodrugs could be delivered across intestinal epithelial cells in their intact form, which is essential to reduce the cytotoxicity to enterocytes for anticancer oral prodrugs. The $t_{1/2}$ values of two OCTN2-targeting prodrugs in plasma were roughly 4-fold shorter compared with that in hepatic homogenate (Figure 3), indicating that the primary bioactivation site was the plasma and then the liver.

An ideal prodrug should exhibit excellent stability in the GI tract before interaction with OCTN2 and then must be converted to the parent drug in the systematic circulation. In general, the ester bond is not very stable to enzymatic hydrolysis[14]. For example, 5'-O-L-phenylalanyl-decitabine is rapidly hydrolyzed in intestinal fluid, with a very short half-life (95 min)[15]. In this study, OCTN2-targeting gemcitabine prodrugs showed excellent enzymatic stability, thereby reducing intestinal degradation to gemcitabine and increasing the targeting delivery, very consistent well with the previous study of the valproate amide prodrug of gemcitabine[4].

Contribution of Nucleoside Transporter-1 (hENT1) to the Oral Absorption

To investigate the possible contribution of hENT1 to the oral absorption of the targeted prodrugs (GSC and GHC), a competitive inhibitor dipyridamole was used to study the cellular uptake of prodrugs in Caco-2 cells, which are known to express hENT1[16]. Figure S7 showed that 2.5 mM dipyridamole did not affect the cellular uptake of GSC and GHC, confirming that these prodrugs entered cells in a nucleoside

transporter-independent manner.

Cellular uptake mechanism of OCTN2-targeting oral prodrugs

The uptake of GSC and GHC by Caco-2 cells (naturally express OCTN2) was reduced by 2- to 10-fold where Na^+ in medium was replaced with N-methyl-D-glucamine (Figure 4C), whereas no effect of Na^+ on GS and gemcitabine was observed (Figure 4D). The results suggested that the cellular uptake of the targeted prodrugs was in a Na^+-dependent manner. Moreover, the uptake of GHC and GSC was significantly higher at 37 °C than 4 °C, while GS and gemcitabine were not affected, indicating the involvement of transporter-mediated transport (Figure 4E).

To confirm the contribution of OCTN2 on the transport of the targeted prodrugs, OCTN2 gene transfected HEK293 (HEK293-OCTN2) cells were used. As expected, the uptake of GSC and GHC was, respectively, 3- to 8-fold higher in HEK293/OCTN2 than HEK293 cells, but there was no significant difference in gemcitabine between the two cells (Figure 5), indicating that the targeted prodrugs was specifically taken up by the cells via interaction with OCTN2. To further confirm that the active transport was mediated by OCTN2, the competitive experiments between the targeted prodrugs and L-carnitine were investigated. As shown in Figure 4F, the uptake of L-carnitine was decreased by 42% to 70% in the presence of 100 μM the targeted prodrugs. Moreover, the cellular uptake of the targeted prodrugs was significantly reduced (by 2.2-3.7 fold) in the presence of 100 μM L-carnitine, a typical substrate of OCTN2 (Figure 4A), but there was no effect for GS and gemcitabine (Figure 4B). However, the uptake amounts of the targeted prodrugs were

not affected by the presence of palmitoyl-L-carnitine, a carnitine analogue but not substrate of OCTN2 (Figure 4A). Therefore, these data suggested that the targeted prodrugs were taken up into Caco-2 cells via OCTN2 protein.

In addition, GHC (6-carbon length linker) exhibited 1.8- to 2.5-fold better uptake in Caco-2 cells than GSC, GOC and GDC (4, 8 and 10-carbon length linker). Kinetic analysis showed that K_m value of GHC was roughly 2.2 - 3.9 folds lower than other targeted prodrugs, but their V_{max} values were similar (0.2013 nmol/mg/10 min-0.4344 nmol/mg/10 min), suggesting the increased cellular uptake of GHC was due to an increase in its binding affinity (Figure 6). These results indicated that the fatty acid chain length has a determining effect on the affinity of the substrate toward OCTN2.

Computational docking studies

The crystal structure of OCTN2 protein has not been resolved, so we chose a computational model of hOCTN2. Homology model of OCTN2 was constructed similar to that described previously for OCT1[17]. The sequence of human OCTN2 was obtained from the Uniprot database (entry O76082; http://www.uniprot.org), and GlpT (PDB entry: 1PW4) as template[18]. The carnitine (S467) binding site in the computational model of hOCTN2 was used to investigate interactions between transporter and prodrugs. From a thermodynamic view, a negative free energy ($\Delta G<0$) indicates a favorable interaction system. The calculated binding energy values were -3.37 KJ/mol for GHC and -2.23 KJ/mol for GSC, demonstrating that GHC had a stronger interaction with OCTN2 than GSC. Moreover, due to long chain lipophilic linkage, the oxygen atom on the pyridine ring of GHC formed H-bond with Gly206

residue, which significantly contributes to stabilize the conformations of protein-prodrugs complex (Figure 7). The trend in the binding affinities was consistent with the above cellular experiments.

Caco-2 Monolayer Permeability

The apparent transcellular permeability of gemcitabine and its prodrugs across Caco-2 monolayer is shown in Figure 8. The permeability of the targeted prodrugs was significantly higher in the AP→BL direction in comparison to the BL→AP direction, whereas there was no significant difference for gemcitabine and GS, indicating active transport of the prodrugs. All the targeted prodrugs increased permeability of AP→BL direction by 5-fold to 15-fold, compared with gemcitabine, and the permeability of GS was comparable with that of gemcitabine. Given the low cellular uptake of GS in Figure 8D, poor permeability may be due to high retention in the lipid bilayer of the plasma membrane. To confirm the contribution of OCTN2 to the permeability of the prodrugs, a typical substrate L-carnitine was co-incubated with the targeted prodrugs. The permeability of the targeted prodrugs across Caco-2 monolayer was reduced by 1.6- to 3.6-fold in the presence of 100 μM L-carnitine and was not affect affected by the presence of 100 μM palmitoyl-L-carnitine, indicating that the improved permeability was mediated by OCTN2. Compared with 5'-D-Phenylalanyl-gemcitabine in a previous study[6], OCTN2-targeting oral prodrugs exhibited higher permeability (15-fold VS 4.5-fold), indicating that the transport ability of OCTN2 was better than that of PepT1. More interestingly, GHC (6-carbon length linker) exhibited a 1.7 fold increase in P_{app} value compared to GSC (4-carbon

length linker). But, GOC and GDC (8 and 10-carbon length linker) exhibited a 1.7- and 3-fold lower P_{app} value compared to GHC. Thus, it seems that the length of linker play a crucial role in the performance of permeability. GHC exhibited a significantly higher permeability than other targeted prodrugs, probably due to optimal chain length of the linkage that facilitates an increased interaction of GHC with the binding domain of OCTN2 transporter protein.

Correlation of Lipophilicity and Permeability

To explore the correlation between the membrane permeability and lipophilicity, the octanol-water distribution coefficients (log P) were determined at pH 7.4 and 37 °C using the n-octanol/water shake flask method (Table S1). GS had the highest log P value and gemcitabine had the lowest. However, the lipophilicity was not correlated with the high Caco-2 membrane permeability of the prodrugs (Figure 9), indicating that, rather than passive diffusion, another transcellular mechanism is responsible for the high permeation rates of OCTN2-targeting prodrugs.

In situ single-pass perfusion

The effective permeability (P_{eff}) and the absorption rate (K_a) of gemcitabine and the prodrugs were determined using the in situ single-pass intestinal perfusion system in rats[19]. The K_a and P_{eff} values of GSC and GHC were generally higher than those of gemcitabine in whole intestinal segments (Figure 10 and Table 1). The P_{eff} and K_a values of GS were significantly lower than those of GSC and GHC, suggesting that the contribution of passive transport for GSC and GHC was low. The P_{eff} values of GSC and GHC were reduced 25- and 11-fold in the presence of L-carnitine,

respectively (Figure S8), agreeing well with the results of Caco-2 cellular permeability study. In addition, only trace amounts of gemcitabine were observed in the perfusate, suggesting that OCTN2-targeting oral prodrugs are stable within the GI tract.

Cytotoxicity

In vitro cytotoxicity of all the prodrugs and gemcitabine was evaluated on BxPC-3 cells and Caco-2 cells with the 3-[4, 5-dimethylthiazol-2-yl]-2, 5-diphenyltetrazolium bromide (MTT) assay kit. The half inhibitory concentration (IC_{50}) values were calculated and listed in Table S2. As reflected in Figure S9A, the OCTN2-targeting prodrugs caused significant cytotoxicity in BxPC-3 cells in a dose-dependent manner after 48 h incubation. Compare to gemcitabine, the targeted prodrugs showed equivalent cytotoxicity, indicating that the amide-type prodrugs can rapidly release active gemcitabine molecules to produce cytotoxicity. To examine the possible involvement of OCTN2, we next compared the in vitro cytotoxicity of GHC between the presence and the absence of 100 μM L-carnitine in Caco-2 cells. As shown in Figure S9B, GHC was less effective in killing cancer cells in the presence of L-carnitine and the IC_{50} value of GHC was significantly increased by 8 fold, but there was no effect for gemcitabine. This finding showed that the cytotoxic of targeted prodrug was dependent on the effective uptake into tumor cells via OCTN2. In addition, the in vitro cytotoxicity results of GHC showed that much lower cytotoxicity in Caco-2 cells than BxPC-3 cells (IC_{50} 40.9 VS 0.32 μM), probably since Caco-2 cells were usually resistant to chemotherapy agents[20] and gemcitabine had weaker

activity in colon cancer cells. These results also indicated that there was no toxicity of GHC in intestinal epithelial cells.

Oral Pharmacokinetic Evaluation

The plasma concentration-time profiles of gemcitabine, a non-targeting prodrug (GS) and OCTN2-targeting prodrugs (GSC, GHC, GOC and GDC) were compared after oral administration to rats (an equivalent gemcitabine dose of 50 mg/kg). The plasma concentration of prodrugs and gemcitabine were simultaneously determined using UPLC-MS/MS method. Figure 11 summarized the overall concentration-time curves of all the drugs, and table 2 listed the pharmacokinetic parameters. The detailed pharmacokinetic profiles of the prodrugs and gemcitabine are shown in Figure S10-S15. All the targeted prodrugs were rapidly absorbed after oral administration and the absolute oral bioavailability ranged from 4 % to 16 %, respectively. The bioavailability of the targeted prodrugs was about 1.2-fold to 4.9-fold greater than that of gemcitabine (3.2 %). Also, the half-lives of the targeted prodrugs were about 3-fold greater than that of gemcitabine. The pharmacokinetic results suggested that high membrane permeability together with enzymatic stability markedly improved the oral bioavailability of gemcitabine. By contrast, GS showed similar oral bioavailability to gemcitabine, indicating poor permeability and rapid degradation by CD which probably limited its oral absorption.

To evaluate the role of OCTN2 in the oral absorption of GSC in vivo, competitive inhibition studies were involving co-administration with L-carnitine. The absolute bioavailability of GSC decreased from 12% to 6% in the presence of

L-carnitine (P<0.05) (Table S3). These results further confirmed the improved oral bioavailability was due to OCTN2-mediated delivery. In addition, OCTN2 is expressed in the brush border membranes of the proximal tubule cells and is responsible for efficient reabsorption of filtered L-carnitine and acetylcarnitine (AC) [18]. Thus, the targeted prodrugs may be reabsorbed into the system circulation mediated by OCTN2, which probably contribute to the increased long residence time of these targeted prodrugs. More importantly, GHC exhibited a significantly prolonged plasma half-lives and the highest oral bioavailability among the targeted prodrugs, and the longer chains (8-10 carbons) did not help improve pharmacokinetic behavior of gemcitabine through OCTN2. Therefore, the linker lengths are of a crucial role in the performance of OCTN2-targeting oral prodrug strategy due to the fatty acid length could affect the affinity of the substrate toward transporter, in good agreement with the results of the cellular study.

To explore the bioactivation mechanism, systemic and portal vein plasma concentrations of GSC and gemcitabine were determined. GSC was able to cross the intestinal epithelium cells primarily in intact form, with a mean GSC concentration of 2456 ng/mL while the mean gemcitabine concentration was 199 ng/mL at 2h in portal blood, suggesting that GSC remained stable after the intestinal absorption process. Moreover, the mean concentration for gemcitabine in portal vein was only 10% that of gemcitabine in the jugular vein at 2h, indicating that bioactivation mainly occurred in the blood and liver. This result was different from our previous study of amino acid ester-based valylcytarabine and valyldidanosine[21, 22], in which over 98% of prodrug

bioactivation occurred in the GI tract and intestinal cells. Also, our previous report indicated that the relatively rapid degradation in the GI tract and intestinal cells was unfavourable to improve the oral bioavailability and to reduce the intestinal toxicity of transporter-targeting prodrugs. By contrast, the introduction of an amide bond contributed to the improvement in the stability of the prodrug, which changed the bioactivation site in vivo. Therefore, the relatively good chemical and enzymatic stability in the GI tract appears to help the oral bioavailability and to maintain the minimal intestinal toxicity of OCTN2-targeting oral prodrugs.

Tissue distribution study

The tissue distribution was investigated in mice after a single oral administration of 102 mg/kg of GHC (an equivalent gemcitabine dose of 50 mg/kg). The concentrations of gemcitabine in vital organs were determined at 0.16 h, 0.5 h and 2 h after administration (Figure 12). The tissue distribution results demonstrated that GHC was mainly distributed in mice's spleen, heart and lung at 0.5 h, but was rapidly decreased after 2 h, indicating good safety of GHC in vital organs in the body.

In vivo safety studies

OCTN2 is widely expressed in all organs, including heart, liver, spleen, lung and kidney, which may increase drug uptake and thus produce organ toxicity. In vivo safety studies was carried out on heart, liver, spleen, lung and kidney tissue after continuous administration of GHC for 14 days (50 mg/kg/day) using Hematoxylin and eosin (H&E) histological analysis. Compared to PBS group, the microstructures of organs from GHC treated mice were normal (Figure 13). No evidence of hydropic

degeneration, inflammatory infiltrates and fibrosis was observed in cardiac muscle, hepatocytes, spleen, lung and kidney samples, indicating that there was no toxicity of GHC in mice at short exposure duration, probably due to low tissue distribution and rapid clearance in various tissues.

CONCLUSIONS

OCTN2-targeting oral prodrugs of gemcitabine simultaneously increased the permeability and stability in comparison with PepT1-targeting prodrugs and lipophilized prodrugs, resulting in higher oral bioavailability. No toxicity in mice was observed after short exposure duration (14 days) following oral administration of OCTN2-targeting gemcitabine prodrug. In particular, the hexane diacid linkage exhibits a 2.2-fold increased OCTN2 affinity and a 1.3-fold increase in oral bioavailability, compared with the succinic acid linkage. These findings support the notion that in addition to PepT1, OCTN2 transporter can be used as a novel target to deliver gemcitabine by the most practical oral route. Furthermore, the fatty acid linkage chain length can modify the affinity of the substrate toward transporter. We have shown that OCTN2-targeting oral prodrugs strategy may be feasible for the oral deliver other antitumor agents.

EXPERIMENTAL SECTION

Chemicals

Gemcitabine (98.8% purity) was purchased from Nanjing Chemlin Chemical Industry Co., Ltd (Jiangsu, Nanjing, PR China); L-carnitine, isobutyl chlorocarbonate, triethylamine, succinic anhydride, adipic anhydride, octandioic acid, decanedioic acid, sulfoxide chloride, 1,4-dioxane, DMF, benzyl bromide were supplied by Sigma Aldrich and used without further purification; tetrahydrouridine (THU), a cytidine deaminase inhibitor, was purchased from J & K Scientific (HPLC grade); Caco-2 cells were obtained from ATCC and HEK293 cells were kindly provided by Dr Xiu-Lin YI (Tian Jin Institute Research Pharmaceutical Corporation); L-carnitine-succinic-gemcitabine (GSC), L-carnitine-hexylic-gemcitabine (GHC), L-carnitine-octanedioic-gemcitabine (GOC), L-carnitine-decanedioic-gemcitabine (GDC), and succinic-gemcitabine (GS) were synthesized in Shenyang Pharmaceutical University (Shenyang, China).

Synthesis of OCTN2-targeting prodrugs of gemcitabine

All compounds were analyzed by ^{1}H NMR and MS. The purity of OCTN2-targeting prodrugs was ≥95% as determined by HPLC.

Synthesis of GSC

A mixture of compound 2 (1.2 g, 0.003 mol), gemcitabine (0.78 g, 0.003 mol), isobutyl chloroformate (0.6 g, 0.045 mol), triethylamine (TEA, 0.3 g, 0.003 mol) and DMF (10mL) was stirred overnight at 60 °C, under an argon atmosphere. The solvent was evaporated, and the residue was purified by column chromatography on a silica

gel, eluting with methanol in dichloromethane (gradient 5-10 %). The pure intermediate was dissolved in methanol, and then Pd/C (10 %) was added. The mixture was stirred under H_2 at room temperature for 15 minutes and filtered. The solvent was evaporated, and product was collected in a vacuum. Yield: 67 % of a white powder. $C_{20}H_{28}F_2N_4O_9$, MS (ESI)：m/z = 507.2 [M+H$^+$]. HPLC purity: t_R = 7.9 min, 98.2 %. ^{1}H NMR (400 MHz, DMSO-d6): δ 10.86 (d, J = 286.0 Hz, 2H), 8.31 (d, J = 7.6 Hz, 1H), 7.20 (d, J = 7.5 Hz, 1H), 6.48 (s, 1H), 6.15 (t, J = 7.1 Hz, 1H), 5.86 (dd, J = 13.9, 4.8 Hz, 2H), 5.39 (s, 1H), 5.25 (s, 1H), 4.28 – 4.03 (m, 8H), 3.86 (d, J = 8.6 Hz, 1H), 3.76 (s, 1H), 3.61 (ddt, J = 16.3, 12.4, 7.8 Hz, 10H), 3.36 (d, J = 19.8 Hz, 10H), 3.08 (s, 9H), 2.75 (s, 2H), 2.56 (dd, J = 11.9, 4.5 Hz, 4H).

Synthesis of GHC

A mixture of compound 3(1.2 g, 0.003 mol), gemcitabine (0.78 g, 0.003 mol), isobutyl chloroformate (0.6 g, 0.045 mol), triethylamine (TEA, 0.3 g, 0.003 mol) and DMF (10 mL) was stirred overnight at 60 °C, under an argon atmosphere. The solvent was evaporated, and the residue was purified by chromatography on a silica-gel column, eluting with methanol in dichloromethane (gradient 5-10 %). The pure intermediates were dissolved in methanol, and then Pd/C (10 %) was added. The mixture was stirred under H_2 at room temperature for 15 minutes and filtered. The solvent was evaporated, and product was collected in a vacuum. Yield: 35 % of a white powder. $C_{22}H_{32}F_2N_4O_9$, MS, (ESI)：m/z = 535.3 [M+H$^+$]. HPLC purity: t_R = 8.5 min, 97.4 %. ^{1}H NMR (400 MHz, D_2O) δ 8.24 (d, J = 7.6 Hz, 1H), 7.42 (d, J = 7.6 Hz, 1H), 6.28 (t, J = 7.3 Hz, 1H), 5.64 (d, J = 6.3 Hz, 1H), 4.39 (td, J = 12.0, 8.9 Hz, 1H),

4.18 – 4.10 (m, 1H), 4.04 (s, 1H), 3.94 – 3.82 (m, 2H), 3.65 (s, 1H), 3.36 (s, 1H), 3.22 (d, J = 15.9 Hz, 9H), 2.60 – 2.38 (m, 5H), 1.77 – 1.58 (m, 4H).

Synthesis of GOC

A mixture of compound 4(1.23 g, 0.003 mol), gemcitabine (0.78 g, 0.003 mol), isobutyl chloroformate (0.6 g, 0.005 mol), triethylamine (TEA, 0.3 g, 0.003 mol) and DMF (10mL) was stirred overnight at 60 °C, under an argon atmosphere. The solvent was evaporated, and the residue was purified by chromatography on a silica-gel column, eluting with methanol in dichloromethane (gradient 5-10 %). The pure intermediates were dissolved in methanol, and then Pd/C (10 %) was added. The mixture was stirred under H_2 at room temperature for 15 minutes and filtered. The solvent was evaporated, and product was collected in a vacuum. Yield: 42 % of a white powder. $C_{24}H_{36}F_2N_4O_9$, MS (ESI)**:** m/z = 563.2 [$M+H^+$]. HPLC purity: t_R = 10.2 min, 98.2 %. ^{1}H NMR (400 MHz, DMSO-d6) δ 11.02 (s, 1H), 8.29 (d, J = 7.5 Hz, 1H), 7.38 (q, J = 2.8, 2.3 Hz, 1H), 7.28 (d, J = 7.6 Hz, 1H), 6.16 (d, J = 7.5 Hz, 1H), 5.47 (d, J = 26.2 Hz, 1H), 4.20 (dt, J = 13.0, 6.4 Hz, 1H), 3.89 (d, J = 8.0 Hz, 1H), 3.80 (d, J = 12.8 Hz, 2H), 3.66 (dd, J = 12.8, 3.4 Hz, 2H), 3.14 (d, J = 19.3 Hz, 9H), 2.60 (s, 2H), 2.41 (t, J = 7.3 Hz, 2H), 2.31 (d, J = 8.1 Hz, 2H), 1.53 (s, 4H), 1.27 (s, 4H).

Synthesis of GDC

A mixture of compound 4(1.77 g, 0.003 mol), gemcitabine (0.78 g, 0.003 mol), isobutyl chloroformate (0.6 g, 0.005 mol), triethylamine (TEA, 0.3 g, 0.003 mol) and DMF (10 mL) was stirred overnight at 60 °C, under an argon atmosphere. The solvent

was evaporated, and the residue was purified by chromatography on a silica-gel column, eluting with methanol in dichloromethane (gradient 5-10 %). The pure intermediates were dissolved in methanol, and then Pd/C (10 %) was added. The mixture was stirred under H_2 at room temperature for 15 minutes and filtered. The solvent was evaporated, and product was collected in a vacuum. Yield: 47 % of a white powder. $C_{26}H_{40}F_2N_4O_9$, MS (ESI)：m/z = 591.3 [M+H$^+$]. HPLC purity: t_R = 11.3 min, 97.8 %. 1H NMR (400 MHz, DMSO-d6) δ 12.73 (s, 1H), 10.99 (s, 1H), 8.28 (d, J = 7.6 Hz, 1H), 7.28 (d, J = 7.5 Hz, 1H), 6.40 (s, 1H), 6.16 (d, J = 7.5 Hz, 1H), 5.45 (s, 1H), 4.21 (d, J = 10.8 Hz, 1H), 3.91 – 3.88 (m, 1H), 3.82 (s, 2H), 3.68 (d, J = 3.5 Hz, 2H), 3.12 (s, 9H), 2.69 (d, J = 4.7 Hz, 2H), 2.40 (d, J = 7.3 Hz, 2H), 2.25 (t, J = 7.4 Hz, 2H), 1.53 (d, J = 6.5 Hz, 4H), 1.25 (s, 8H).

Synthesis of GS

A mixture of succinic anhydride (0.2 g, 0.002 mol), gemcitabine (0.78 g, 0.003 mol), triethylamine (TEA, 0.1 g, 0.001 mol) and DMF (10 mL) was stirred overnight at 60 °C, under an argon atmosphere. The solvent was then evaporated, and the residue was purified by preparative HPLC. Yield: 75 % of a white powder. $C_{13}H_{17}F_2N_3O_5$, MS (ESI)：m/z = 334.1 [M+H$^+$]. HPLC purity: t_R = 13.5 min, 97.5 %. ^{1}H NMR (400 MHz, DMSO-d6): δ 10.99 (s, 2H), 8.26 (d, *J* = 7.6 Hz, 2H), 7.39 (d, *J* = 24.9 Hz, 2H), 7.29 (d, *J* = 7.6 Hz, 2H), 6.15 (dd, *J* = 15.6, 8.0 Hz, 3H), 5.78 (d, *J* = 7.4 Hz, 1H), 4.25 - 4.10 (m, 3H), 3.88 (d, *J* = 8.5 Hz, 2H), 3.77 (dd, *J* = 18.8, 12.3 Hz, 4H), 3.68 - 3.59 (m, 3H), 2.38 (t, *J* = 7.3 Hz, 4H), 1.58 - 1.51 (m, 3H).

Stability

Plasma was obtained from rats and stored at -80 °C until required. Hepatic and intestinal samples were washed with physiological saline, and 0.3 g tissue (weighed accurately) was mixed with 1mL of physiological saline then homogenized for 1 min. After centrifuging at 13,000 rpm at 4 °C for 5 min, the supernatant was stored at -80 °C until required.

The chemical stability of GS, GSC and GHC were tested in different pH phosphate buffers (pH 1.2, 6.8, 7.4) at 37 °C for 24 h. Drug solutions were prepared by dissolving the prodrugs in buffer to obtain a concentration of 5 μM. In addition, the enzymatic stability was determined in rat plasma, 20% rat hepatic homogenate and 20% rat intestinal homogenate at 37°C 24 h. The prodrugs were added to the plasma, rat hepatic and intestinal homogenate to obtain a final concentration of 5 μM. At the appropriate intervals, samples were collected and then analyzed by HPLC. The degradation half-lives were calculated using the equation:

$$t_{1/2}=0.693/k$$

Caco-2 Permeability

For transcellular transport studies, Caco-2 cells were grown on 12-well polycarbonate filter inserts (0.4 μm pore size, area 1.12 cm^2, Corning, NY) at a density of 1.0×10^5 cells/well and cultured in MEM for 21 days. The transepithelial electrical resistance (TEER) over than 250 $\Omega \cdot cm^2$ were used for the experiment. The apparent permeability coefficients (P_{app}) were determined for the AL→BP and BP→AL directions with and without the presence of 100 μM L-carnitine. Drug solutions were prepared in Han's balanced salt solution (HBSS) to obtain a final concentration

of 25 μM. For AL→BP transcellular transport, HBSS buffer containing the drugs was added to the apical side and free HBSS buffer to the basolateral side. For BP→AL transcellular transport, the drug solution was added to the basolateral side and free HBSS buffer to the apical side. The samples were collected from the apical side or basolateral side at 15, 30, 45, 60, 90, and 120 min at 37 °C. Each experiment was repeated three times. Drug concentrations in both sides were determined by UPLC-MS/MS and P_{app} was calculated using the formula:

$$P_{\mathrm{app}} = \mathrm{d}C_r/\mathrm{d}t \times V_r \times 1/A \times 1/C_0$$

where dC_r/d_t is the steady-state flux across the monolayer (μmol/s), V_r is the receiver volume, A is the surface area of the monolayer (1.13 cm^2), and C_0 is the initial concentration (μM) in the test solution. The concentrations of gemcitabine and its prodrugs were analyzed by UPLC−MS/MS.

Pharmacokinetic Evaluation

All surgical and experimental procedures were performed in accordance with institutional guidelines and approved by the Shenyang Pharmaceutical University Animal Care and Use Committee.

Six groups of Wistar rats (six animals each group) were orally administrated of gemcitabine, GSC, GHC, GOC, GDC and GS at a gemcitabine dose of 50 mg/kg. In addition, GSC was orally co-administered with 40 mM L-carnitine to the rats. Then, serial blood samples were collected at 5, 10, 15, 30 min and 1, 2, 4, 6, 8, 12, 24h. To calculate the absolute bioavailability, gemcitabine was also given intravenously to rats at a dose of 7.5 mg/kg. Serial blood samples were collected at 15, 30 min and 2, 4, 8,

12, 24 h and then transferred to THU-pretreated heparinized tubes (10 mg/mL) after centrifuging at 3000 × g for 15 min. The supernatant of samples were stored at -80 °C until analysis. The absolute bioavailability of gemcitabine was calculated using the following equation:

$$F_{abs} = AUC_{po} \times D_{iv}/AUC_{iv}/D_{po} \times 100\%$$

where F_{abs} is the absolute bioavailability, AUC_{po} is the area under the plasma concentration-time curves of oral administration, D_{iv} is the intravenous administration dose, AUC_{iv} is the area under the plasma concentration-time curves of intravenous administration, and D_{po} is the dose orally administered.

Tissue distribution study

Nine mice were randomly divided into three groups (n = 3) and orally administrated of GHC at the dose of 102 mg/kg. The tissue samples, including heart, liver, spleen, lung, kidney and brain were collected at 0.16, 0.5 and 2 h post-dosing. Tissue samples were washed with physiological saline, and 0.3 g tissue (weighed accurately) was mixed with 1mL of physiological saline then homogenized for 1 min. After centrifuging at 13,000 rpm at 4 °C for 5 min, the supernatant was stored at -80 °C until analysis.

In vivo toxicity study

Two groups of Kunming mice (four animals each group) were orally administrated of GHC or physiological saline (control) at the dose of 102 mg/kg once daily for 14 days. Body weight of each mouse was recorded every other day for 14 days. For histology analysis, mice were sacrificed and the heart, liver, spleen, lung,

and kidney tissue samples were removed, and fixed in 10% buffered formalin immediately, followed by embedding in paraffin, sectioning, and hematoxylin and eosin staining. The histological sections were imaged using an optical microscope.

ASSOCIATED CONTENT

Supporting Information

Additional supporting documents and experimental results are available, including measurement of the Water-Octanol Partition Coefficient (Log P), cell culture, Cellular uptake mechanism study, L-carnitine Uptake Inhibition, Contribution of Nucleoside transporter to the oral absorption, Cytotoxicity, In situ single-pass perfusion, the systemic and portal vein pharmacokinetic evaluation, development of analytical method, statistical analysis and Molecular formula strings and some data (CSV). This material is available free of charge via the Internet at http://pubs.acs.org.

AUTHOR INFORMATION

∗ Corresponding author at: E-mail addresses: sunjin66@21cn.com (J. Sun). Phone: +86 24 23986325; fax: +86 24 23986325.

Notes

The authors declare no competing financial interest

ABBREVIATIONS USED

The organic cation transporter II, OCTN2; cytidine deaminase, CD; 2',2'-difluoro-2'deoxyuridine, dFdU; gastrointestinal, GI; L-carnitine-succinic-gemcitabine, GSC; L-carnitine-hexylic-gemcitabine, GHC; L-carnitine-octanedioic-gemcitabine, GOC; L-carnitine-decanedioic-gemcitabine, GDC; palmitoyl-L-carnitine, PC; succinic-gemcitabine, GS; Nucleoside Transporter-1, hENT1; 3-[4, 5-dimethylthiazol-2-yl]-2, 5-diphenyltetrazolium bromide, MTT; half-maximum inhibitory concentration, IC_{50}; L-carnitine and acetylcarnitine, AC; Hematoxylin and eosin , H&E; tetrahydrouridine, THU; transepithelial electrical resistance, TEER; apparent permeability coefficients, P_{app}; Han's balanced salt solution, HBSS; calculated, calcd; electrospray ionization, ESI; dimethylformamide, DMF; Michaelis constant, K_m; high-performance liquid chromatography, HPLC; hertz, Hz; intravenous, iv; coupling constant (in NMR spectrometry), J; nuclear magnetic resonance, NMR; minute(s), min; milliliter, mL; millimolar, mM; mass spectrometry, Ms; Protein Data Bank, PDB; half-time, $t_{1/2}$.

ACKNOWLEDGMENTS

We are grateful for financial support from the National Natural Science Foundation of China (No. 81473164) and Technology bureau in Shenyang (No. ZCJJ2013402). We are also grateful for financial support from the Project for New Century Excellent Talents of Ministry of Education (No.NCET-12-1015) and Specific Science Foundation of Shenyang Pharmaceutical University (No. ZCJJ2014409).

REFERENCES

1. Pasut, G.; Canal, F.; Dalla Via, L.; Arpicco, S.; Veronese, F. M.; Schiavon, O. Antitumoral activity of PEG-gemcitabine prodrugs targeted by folic acid. *J. Controlled Release* **2008,** *127*, 239-248.

2. Wang, Y.; Fan, W.; Dai, X.; Katragadda, U.; McKinley, D.; Teng, Q.; Tan, C. Enhanced tumor delivery of gemcitabine via PEG-DSPE/TPGS mixed micelles. *Mol. Pharmaceutics* **2014,** *11*, 1140-50.

3. Zhang, Y.; Kim, W. Y.; Huang, L. Systemic delivery of gemcitabine triphosphate via LCP nanoparticles for NSCLC and pancreatic cancer therapy. *Biomaterials* **2013,** 34, 3447-3458.

4. Bender, D. M.; Bao, J.; Dantzig, A. H.; Diseroad, W. D.; Law, K. L.; Magnus, N. A.; Peterson, J. A.; Perkins, E. J.; Pu, Y. J.; Reutzel-Edens, S. M.; Remick, D. M.; Starling, J. J.; Stephenson, G. A.; Vaid, R. K.; Zhang, D.; McCarthy, J. R. Synthesis, crystallization, and biological evaluation of an orally active prodrug of gemcitabine. *J. Med. Chem.* **2009,** *52*, 6958-6961.

5. Zhang, Y.; Gao, Y.; Wen, X.; Ma, H. Current prodrug strategies for improving oral absorption of nucleoside analogues. *Asian J. Pharm. Sci.* **2014,** *9*, 65-74.

6. Tsume, Y.; Incecayir, T.; Song, X.; Hilfinger, J. M.; Amidon, G. L. The development of orally administrable gemcitabine prodrugs with D-enantiomer amino acids: enhanced membrane permeability and enzymatic stability. *Eur. J. Pharm. Biopharm.* **2014,** *86*, 514-523.

7. Song, X.; Lorenzi, P. L.; Landowski, C. P.; Vig, B. S.; Hilfinger, J. M.; Amidon, G. L. Amino acid ester prodrugs of the anticancer agent gemcitabine: synthesis, bioconversion, metabolic bioevasion, and hPEPT1-mediated transport. *Mol. Pharmaceutics* **2005,** *2*, 157-167.

8. Zhang, D.; Bender, D. M.; Victor, F.; Peterson, J. A.; Boyer, R. D.; Stephenson, G. A.; Azman, A.; McCarthy, J. R. Facile rearrangement of N4-(α-aminoacyl)cytidines to N-(4-cytidinyl)amino acid amides. *Tetrahedron Lett.* **2008,** *49*, 2052-2055.

9. Diao, L.; Ekins, S.; Polli, J. E. Quantitative structure activity relationship for inhibition of human organic cation/carnitine transporter. *Mol. Pharmaceutics* **2010,** *7*, 2120-2131.

10. Mo, J. X.; Shi, S. J.; Zhang, Q.; Gong, T.; Sun, X.; Zhang, Z. R. Synthesis, transport and mechanism of a type I prodrug: L-carnitine ester of prednisolone. *Mol. Pharmaceutics* **2011,** *8*, 1629-1640.

11. Napolitano, C.; Scaglianti, M.; Scalambra, E.; Manfredini, S.; Ferraro, L.; Beggiato, S.; Vertuani, S. Carnitine conjugate of nipecotic acid: a new example of dual prodrug. *Molecules* **2009,** *14*, 3268-3274.

12. Pochini, L.; Scalise, M.; Galluccio, M.; Indiveri, C. OCTN cation transporters in health and disease: role as drug targets and assay development. *J. Biomol. Screening* **2013,** *18*, 851-867.

13. Diao, L.; Polli, J. E. Synthesis and in vitro characterization of drug conjugates of l-carnitine as potential prodrugs that target human Octn2. *J. Pharm. Sci.* **2011,** *100*, 3802-3816.

14. Cheon, E. P.; Han, H. K. Pharmacokinetic characteristics of L-valyl-ara-C and its implication on the oral delivery of ara-C. *Acta Pharmacol. Sin.* **2007,** *28*, 268-272.

15. Zhang, Y.; Sun, J.; Gao, Y.; Jin, L.; Xu, Y.; Lian, H.; Sun, Y.; Sun, Y.; Liu, J.; Fan, R.; Zhang, T.; He, Z. A carrier-mediated prodrug approach to improve the oral absorption of antileukemic drug decitabine. *Mol. Pharmaceutics* **2013,** *10*, 3195-3202.

16. Ward, J. L.; Tse, C. M. Nucleoside transport in human colonic epithelial cell lines: evidence for two Na+-independent transport systems in T84 and Caco-2 cells. *Biochim. Biophys. Acta* **1999,** *1419*, 15-22.

17. Perry, J. L.; Dembla-Rajpal, N.; Hall, L. A.; Pritchard, J. B. A three-dimensional model of human organic anion transporter 1: aromatic amino acids required for substrate transport. *J. Biol. Chem.* **2006,**

281, 38071-38079.

18. Huang, Y.; Lemieux, M. J.; Song, J.; Auer, M.; Wang, D. N. Structure and mechanism of the glycerol-3-phosphate transporter from Escherichia coli. *Science* **2003,** *301*, 616-620.

19. Lozoya-Agullo, I.; Zur, M.; Wolk, O.; Beig, A.; Gonzalez-Alvarez, I.; Gonzalez-Alvarez, M.; Merino-Sanjuan, M.; Bermejo, M.; Dahan, A. In-situ intestinal rat perfusions for human Fabs prediction and BCS permeability class determination: Investigation of the single-pass vs. the Doluisio experimental approaches. *Int. J. Pharm.* **2015,** *480*, 1-7.

20. Williamson, E. A.; Boyle, T. J.; Raymond, R.; Farrington, J.; Verschraegen, C.; Shaheen, M.; Hromas, R. Cytotoxic activity of the titanium alkoxide (OPy)(2)Ti(4AP)(2) against cancer colony forming cells. *Invest. New Drugs* **2012,** *30*, 114-120.

21. Sun, Y.; Sun, J.; Shi, S.; Jing, Y.; Yin, S.; Chen, Y.; Li, G.; Xu, Y.; He, Z. Synthesis, transport and pharmacokinetics of 5'-amino acid ester prodrugs of 1-beta-D-arabinofuranosylcytosine. *Mol. Pharmaceutics* **2009,** *6*, 315-325.

22. Yan, Z.; Sun, J.; Chang, Y.; Liu, Y.; Fu, Q.; Xu, Y.; Sun, Y.; Pu, X.; Zhang, Y.; Jing, Y.; Yin, S.; Zhu, M.; Wang, Y.; He, Z. Bifunctional peptidomimetic prodrugs of didanosine for improved intestinal permeability and enhanced acidic stability: synthesis, transepithelial transport, chemical stability and pharmacokinetics. *Mol. Pharmaceutics* **2011,** *8*, 319-329.

Table1 Stability results of prodrugs in different pH phosphate buffers, rat tissue homogenates and plasma at 37 °C.

Media	$t_{1/2}$ (h)		
	GSC	GHC	GS
Phosphate buffer pH 1.2	5.5	4.4	1.0
Phosphate buffer pH 6.8	No hydrolysis	No hydrolysis	45.9
Phosphate buffer pH 7.4	28.4	45.8	10.3
Intestinal homogenates	50.9	78.7	116.5
Hepatic homogenates	15.5	17.4	32.7
Rat plasma	3.7	6.2	1.7

Table 2 Pharmacokinetic parameters of gemcitabine released from targeted prodrugs and gemcitabine, following oral administration of gemcitabine, GS, GSC, GHC GOC and GDC to rats (n=6) at a gemcitabine dose of 50 mg/kg and IV administration of gemcitabine at 7.5 mg/kg, respectively.

PK parameters	$AUC_{0\text{-}24h}$ / (mg/h*l)	$t_{1/2}$/h	C_{max} / mg/l	t_{max}/h
Gemcitabine (iv)	26692.9±5319.3	4.4±1.0	7109.0±3061.2	0.5±0.01
Gemcitabine (p.o.)	5617.8±1355.7	2.3±0.8	1323.6±341.0	1.7±0.6
GS-gemcitabine (p.o.)	9031.6±3299.1	4.3±1.4	1570.1±1063.8	1.9±1.6
GSC-gemcitabine (p.o.)	14916.9±4275.4**	6.2±2.1**	2504.9±844.9	1.0±0.01
GHC-gemcitabine (p.o.)	24324.5±5953.0**	6.8±2.7**	5325.7±2266.2	1.3±0.4
GOC-gemcitabine (p.o.)	11105.0±3854.7**	2.3±1.0	2509.9±691.3	1.2±0.4
GDC-gemcitabine (p.o.)	15907.3±2999.7**	5.4±2.4**	2043.8±490.3	1.8±0.4

[a] $AUC_{0\text{-}t}$: area under the plasma concentration-time profiles from time 0 to the last time point. $t_{1/2}$: elimination half-life. C_{max}: peak plasma concentration. T_{max}: time to reach peak plasma concentration. **P<0.01 compared with gemcitabine.

FIGURES

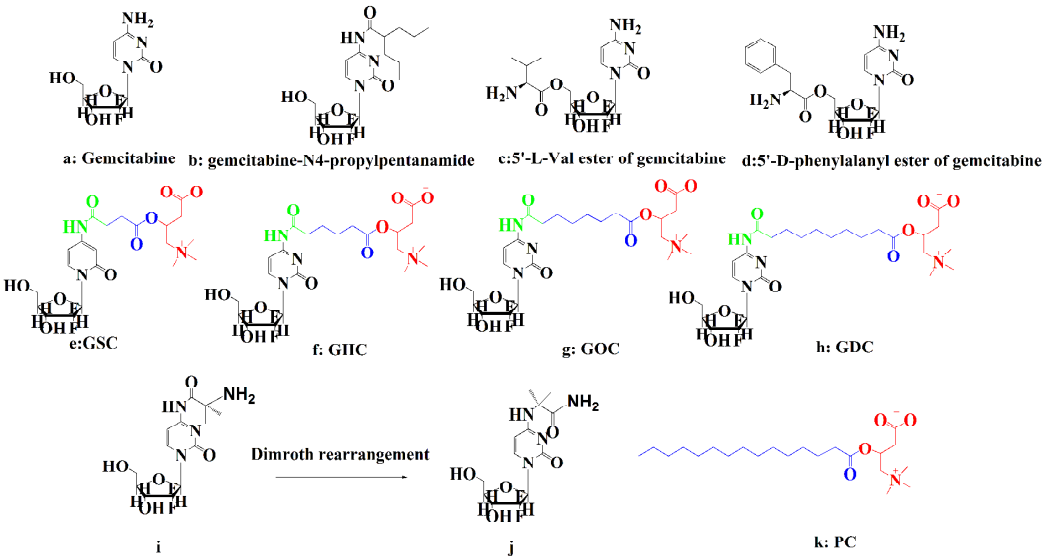

Fig. 1 The Chemical structures of gemcitabine and prodrugs, a: Gemcitabine; b: gemcitabine-N4-propylpentanamide (LY2334737[4]); c: 5'-D-valyl-gemcitabine; d: 5'-D-phenylalanyl-gemcitabine; e: GSC; (f): GHC; (g): GOC; (h): GDC; (i) 4-L-valyl-gemcitabine (j): N-(4-cytidinyl)-L-valyl amide; (k): palmitoyl-L-carnitine (PC).

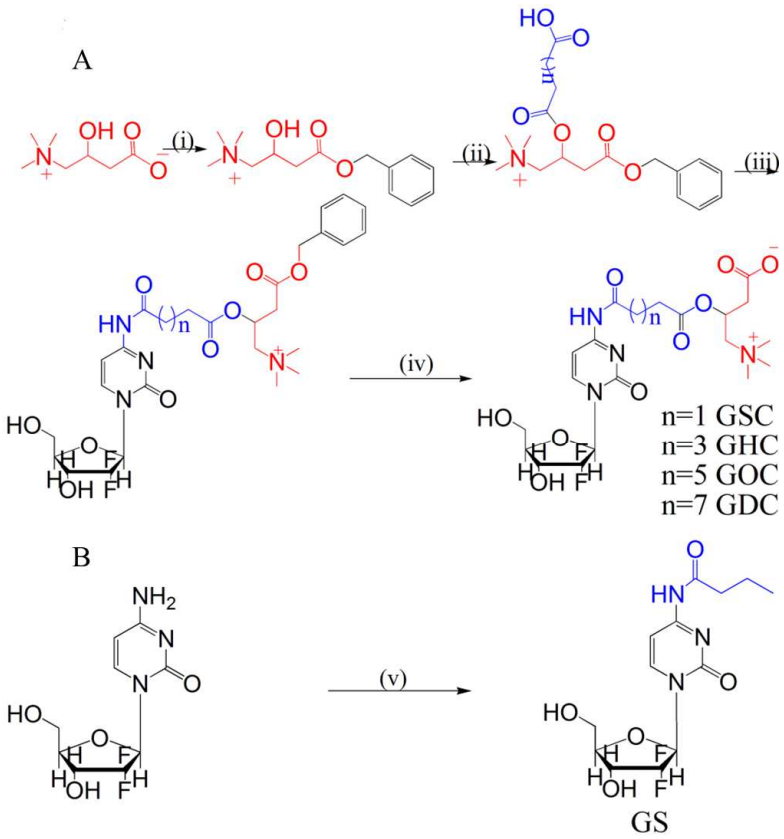

Fig. 2 Synthetic route for preparing prodrugs from gemcitabine: A: synthetic route of GSC, GHC, GOC and GDC, n=1, 3, 5, 7 ; Reagents: (i) Benzyl bromide, DMF, 140°C, 4 h; (ii) Anhydride or diatomic fatty acyl chloride, TEA, DMF, room temperature, 2 h; (iii) Isobutyl chloroformate, TEA, DMF, 60 °C, overnight; (iv) Pd/H_2, room temperature, 10 min; B: synthetic route of GS. (v) Butyric acid, Isobutyl chloroformate, TEA, DMF, 60 °C, overnight.

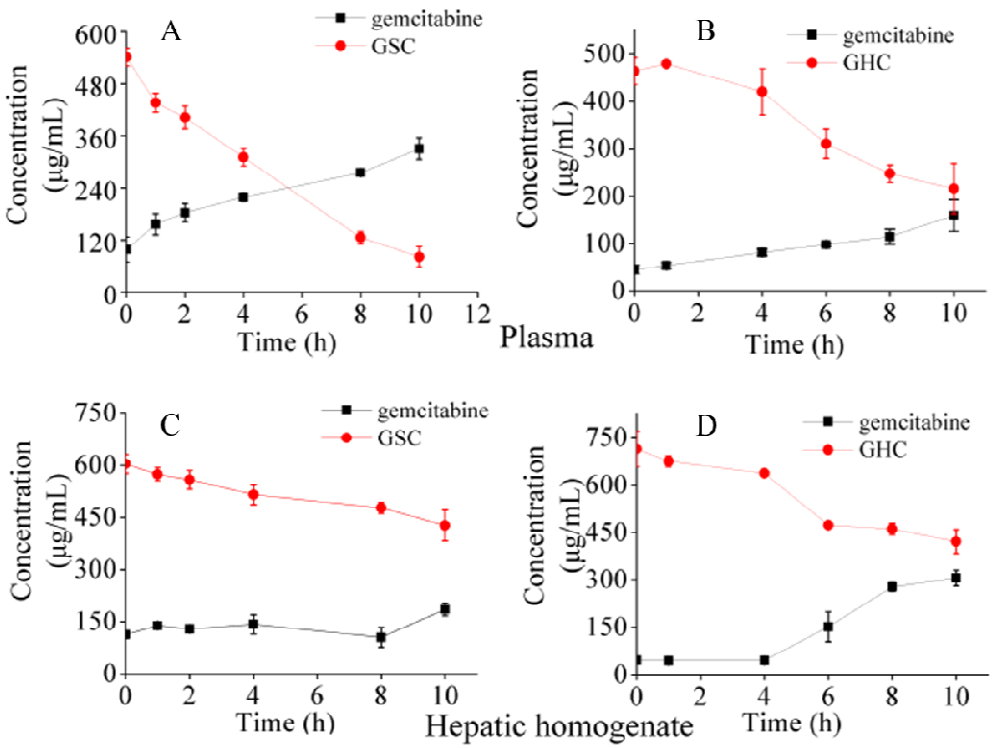

Fig.3 Concentration-time profile for the degradation of targeted prodrugs. A-B: GSC and GHC in rat plasma; C-D: GSC and GHC in hepatic homogenate. The release of gemcitabine from the prodrugs is also shown.

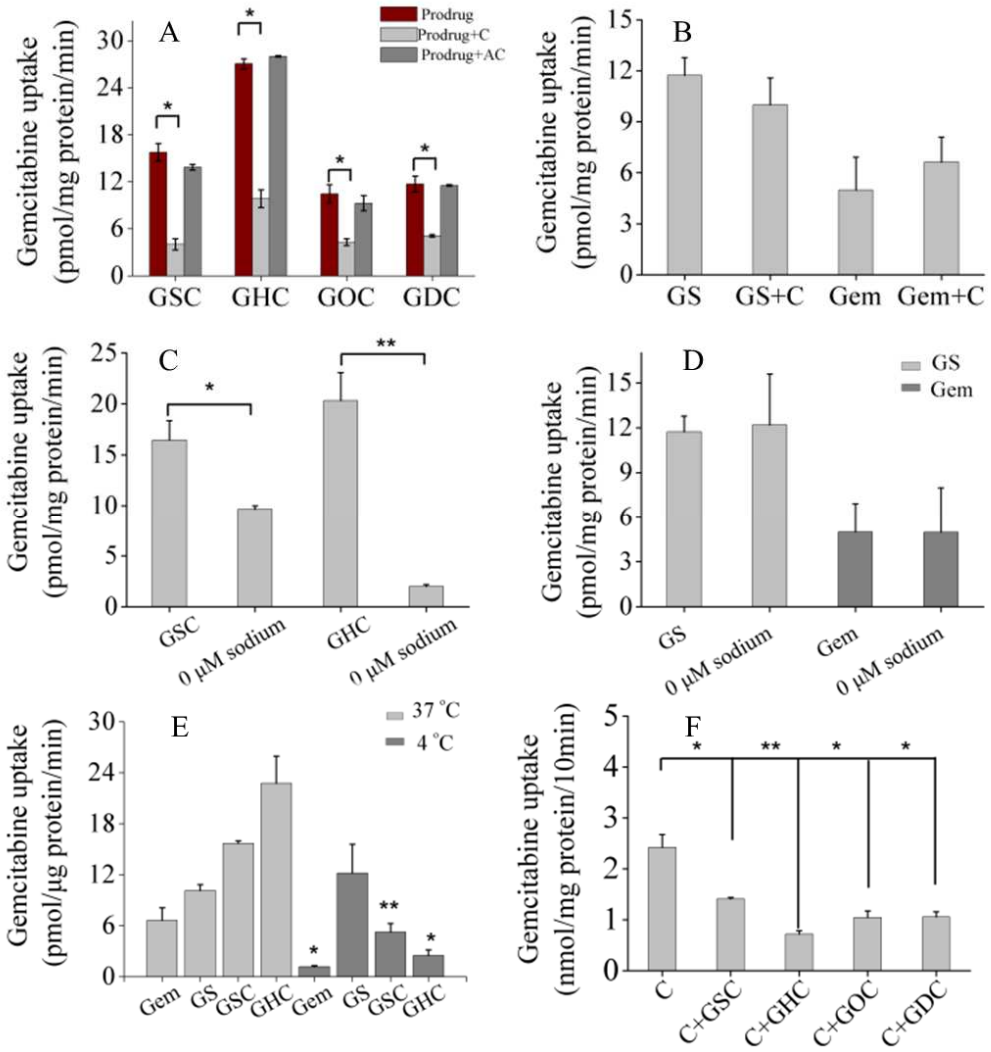

Fig. 4 A: Effect of L-carnitine (C) and palmitoyl-L-carnitine (PC) on the cellular uptake of OCTN2-targeting prodrugs (GSC, GHC, GOC and GDC) in Caco-2 cells; B: Effect of L-carnitine (C) on the cellular uptake of GS and gemcitabine (Gem) in Caco-2 cells; C-D: Effect of extracellular Na^+ on the cellular uptake of prodrugs by Caco-2 cells; E: Effect of temperature on cellular uptake after exposing the Caco-2 cells to gemcitabine, GSC, GHC and GS for 10 min at 37 °C and 4 °C; F: Relative L-carnitine uptake inhibition in Caco-2 Cells by OCTN2-targeting prodrugs. The results in all experiments are expressed as the mean ± SD (n = 3), *P < 0.05 versus control and **P < 0.01 versus control. The inset P values in the figure indicate the significance between groups.

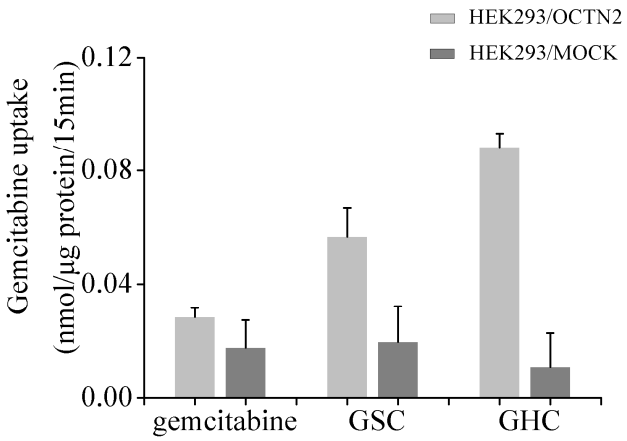

Fig. 5 Uptake of gemcitabine and its prodrugs (GSC and GHC) in OCTN2/HEK293 cells and HEK293 mock cells. OCTN2/HEK293 cells and HEK293 cells were incubated at 37 °C for 15 min with 25 μM gemcitabine, GSC and GHC, respectively (n = 2).

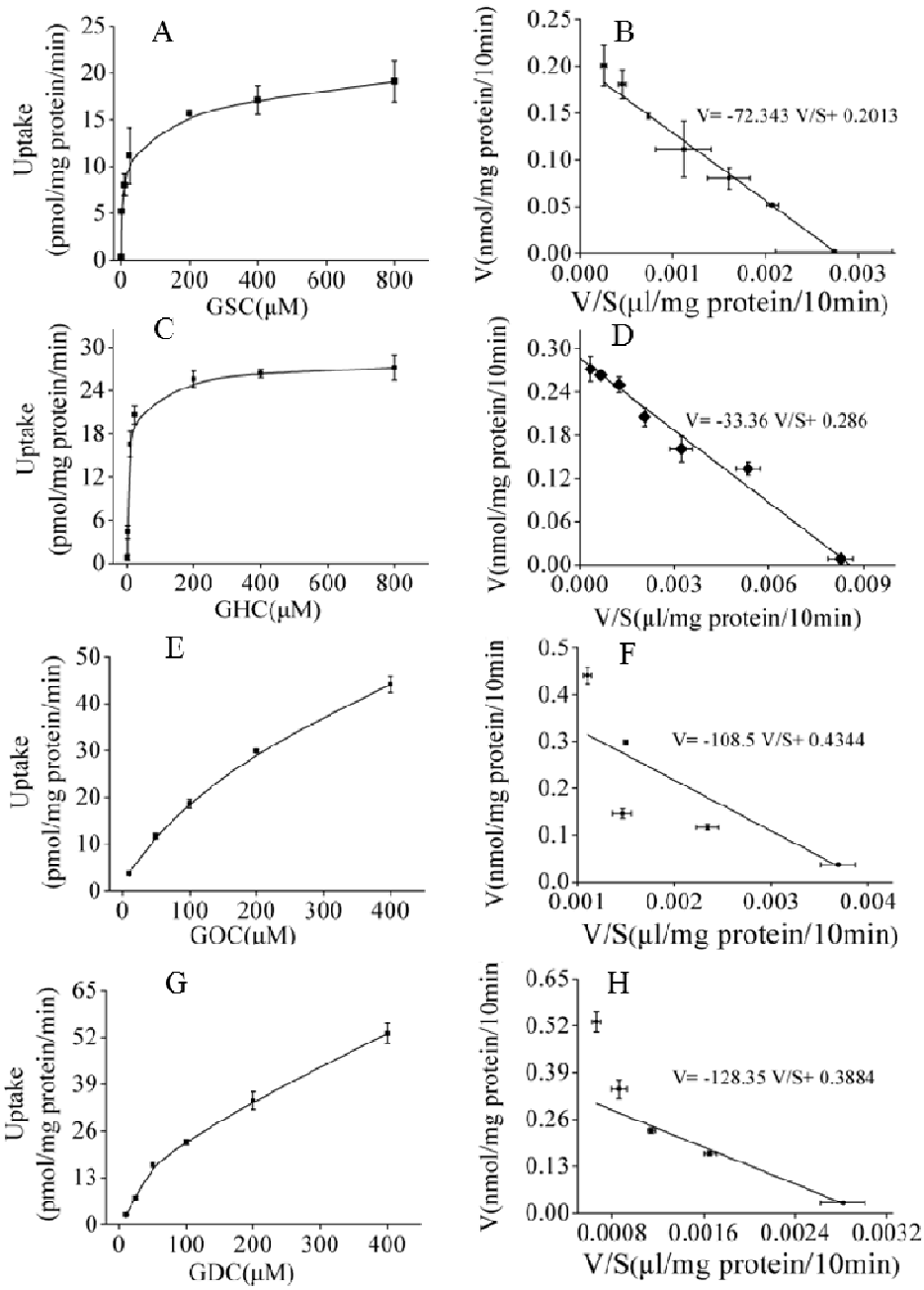

Fig. 6 Concentration-dependent uptake of GSC (A), GHC (C), GOC(E) and GDC (G) in Caco-2 cells; Eadie-Hofstee plot of saturable GSC (B), GHC (D), GOC(F) and GDC (G) by Caco-2 cells. V: uptake rate (pmol/mg of protein/ min); S: prodrugs concentration (μM).

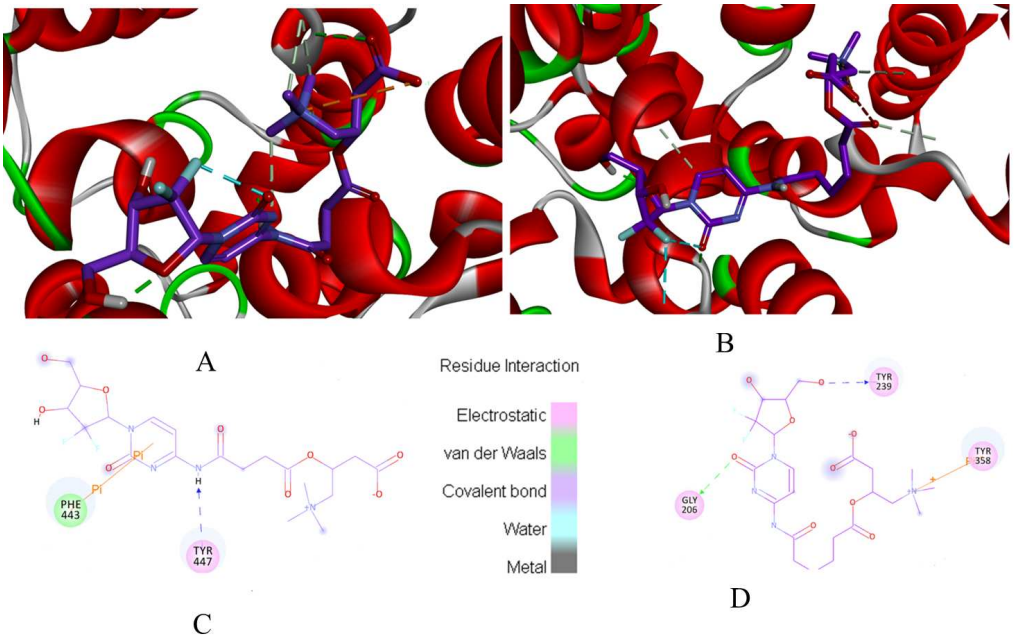

Fig.7 Docking of GSC (a, c) and GHC (b, d) inside the L-carnitine binding site of hOCTN2. The homology modeled structure of hOCTN2 (with PDB code 1PW4 template) is displayed with solid ribbon colored by secondary structure. The ionic-dipole H-bond is shown in green dotted lines, weak H-bonding interaction is shown in blue dotted lines, and π-π interaction is shown in yellow dotted lines.

`

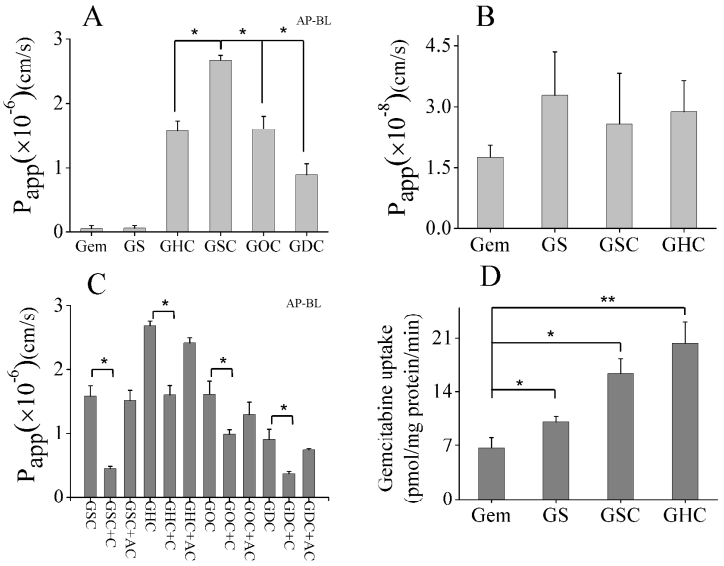

Fig. 8 A: The apical-to-basolateral permeability (P_{app}) for the transport of gemcitabine, GS and OCTN2-targeting prodrugs in Caco-2 cells; B: The basolateral-to-apical permeability (P_{app}) for the transport of gemcitabine, GSC, GHC and GS in Caco-2 cells; C: Effect of Effect of L-carnitine (C) and palmitoyl-L-carnitine (PC) on targeted prodrugs transport in the apical-to-basolateral direction across the Caco-2 cells monolayer; D: The cellular uptake of gemcitabine and its prodrugs by Caco-2 cells. (Mean ± SD, n =3), * P <0.05, compared with control. The inset P values in the figure indicate the significance between groups.

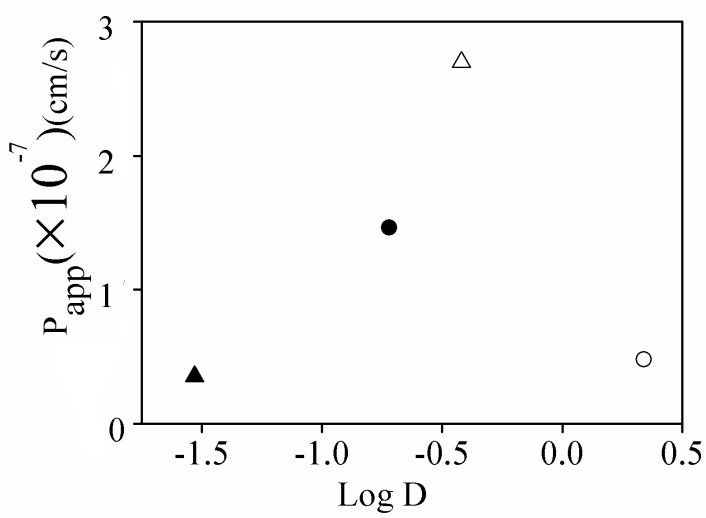

Fig. 9 Log D and Caco-2 permeation rate profile of gemcitabine (▲), GSC (●), GHC (△), and GS (○).

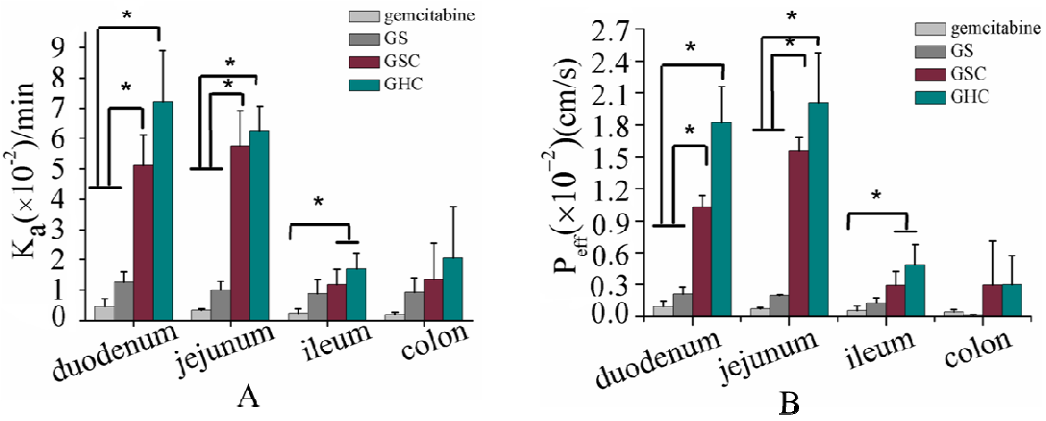

Fig. 10 (a): K_a of gemcitabine, GSC, GHC and GS in four intestinal segments in an in situ SPIP in rats; (b): P_{eff} of gemcitabine, GSC, GHC and GS in four intestinal segments in an in situ SPIP in rats. Permeability was measured in four rat intestinal segments by an in situ single pass perfusion of aqueous solutions of 76 μM gemcitabine, GSC, GHC and GS. (Mean ± SD, n =3), *P <0.05, compared with the control. The inset P values in the figure indicate the significance between groups.

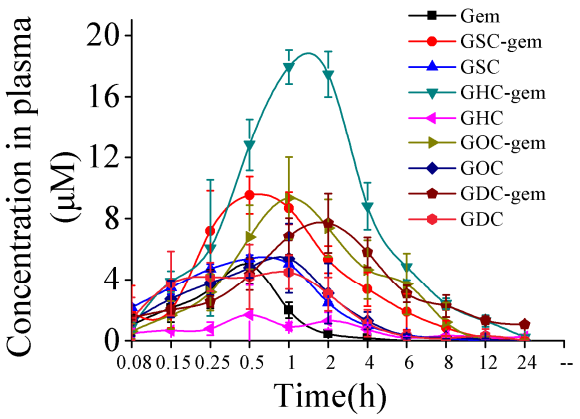

Fig. 11 Plasma profile of gemcitabine, GSC, GHC, GOC and GDC after oral administration of a single dose of 50 mg/kg (calculated as gemcitabine). (The data are expressed as Mean ± SD, n =6).

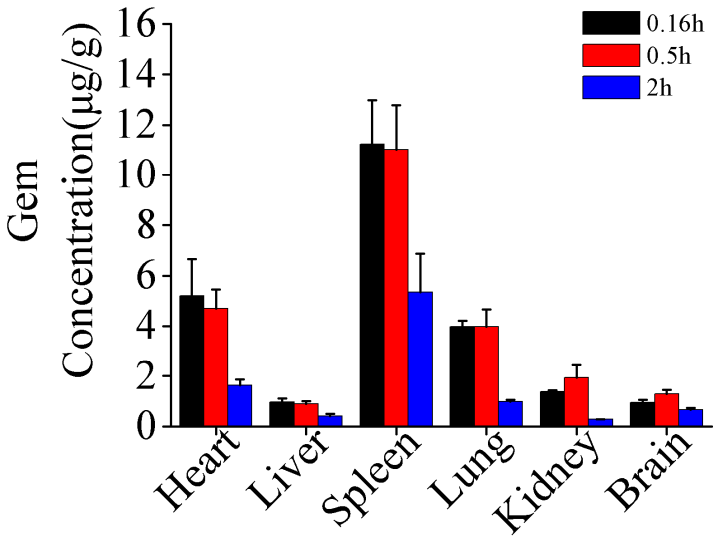

Fig. 12 Tissue Distribution profiles of Gemcitabine in mice tissues at 0.16, 0.5 and 2 h following oral administration of GHC at a single dose of 102 mg/kg (n=3).

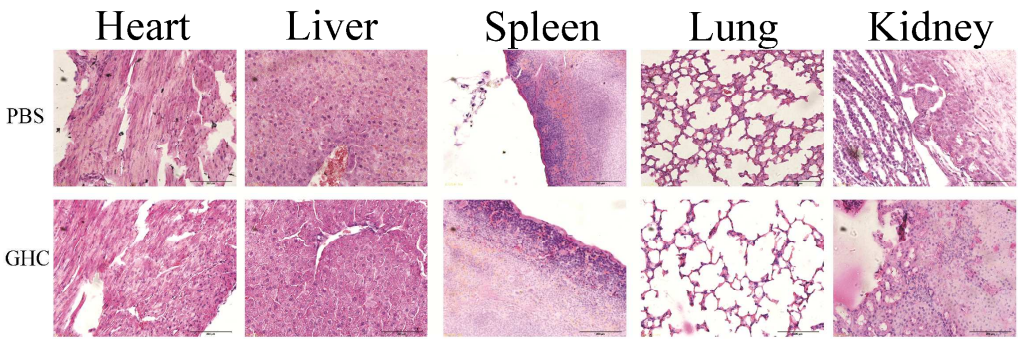

Fig. 13 H&E stained tissue sections from mice after continuous oral administration of GHC (102 mg/kg/day) or PBS for 14 days, respectively. Tissues were harvested from heart, liver, spleen, lung and kidney.

Table of contents graphic